

CLC-3 Chloride Channels in the Pulmonary Vasculature

Joseph R. Hume, Ge-Xin Wang, Jun Yamazaki, Lih Chyuan Ng,
and Dayue Duan

Abstract Volume-sensitive outwardly rectifying anion channels (VSOACs) are expressed in pulmonary artery smooth muscle cells (PASMCs) and have been implicated in cell proliferation, growth, apoptosis and protection against oxidative stress. In this chapter, we review the properties of native VSOACs in PASMCs, and consider the evidence that CIC-3, a member of the CIC superfamily of voltage dependent Cl⁻ channels, may be responsible for native VSOACs in PASMCs. Finally, we examine whether or not native VSOACs and heterologously expressed CIC-3 channels function as bona fide chloride channels or as chloride/proton antiporters.

Keywords Chloride channels • cell volume • pulmonary artery • CIC-3

1 Introduction

Volume-sensitive outwardly rectifying anion channels (VSOACs) are ubiquitously expressed in mammalian cells and play a vitally important physiological role in a variety of cellular functions, including cell volume homeostasis, proliferation, apoptosis, and the regulation of electrical activity.¹ VSOACs have been implicated in a number of these functions in vascular smooth muscle cells (SMCs) as well. For example, the magnitude of VSOAC currents in actively growing SMCs is higher than in growth-arrested or differentiated SMCs, suggesting that VSOACs may be important for SMC proliferation.² There is evidence that pressure-induced depolariza-

J.R. Hume (✉), G. Wang, L. Chyuan Ng, and D. Duan
Department of Pharmacology, Center of Biomedical Research Excellence,
University of Nevada School of Medicine, Reno, NV, 89557, USA
e-mail: jhume@medicine.nevada.edu

J. Yamazaki
Department of Physiological Sciences and Molecular Biology, Fukuoka Dental College,
Fukuoka, Japan

tion and contraction of cerebral artery smooth muscle may be partially mediated by VSOACs.³

Although the exact identification of the proteins responsible for native VSOACs has proven to be elusive, the short isoform of CIC-3 (sCIC-3), a member of the CIC superfamily of voltage-dependent chloride channels, has been proposed to be the molecular correlate of the native VSOAC in some cells, including cardiac myocytes and vascular SMCs.^{4,5} This hypothesis has been corroborated by a series of other independent studies from different laboratories.⁶⁻¹¹ Despite these data, the role of CIC-3 as a constituent of native VSOACs remains controversial.¹²⁻¹⁴ Much of this controversy comes from results reported from the first transgenic CIC-3 global knockout (*CICn3^{-/-}*) mouse produced by Jentsch and coworkers.¹⁵ They reported the apparent presence of native VSOACs in at least two different cell types from *CICn3^{-/-}* mice. However, later experiments using global *CICn3^{-/-}* transgenic mice revealed that the properties of native VSOACs were actually altered in heart, and there appeared to be significant compensatory changes in expression of a variety of other membrane proteins (including upregulation of two other members of the CIC chloride channel family), raising fundamental questions about the usefulness of the global *CICn3^{-/-}* mouse model to assess CIC-3 function.¹⁶ It has been demonstrated that transgenic mice with cardiac-specific overexpression of the human short CIC-3 (hsCIC-3) isoform exhibit enhanced VSOAC currents and accelerated regulatory volume decreases,¹⁷ which is consistent with a molecular role for sCIC-3 in native VSOAC function.

It has been demonstrated that CIC-3 is expressed in human aortic SMCs¹⁸ and pulmonary artery SMCs (PASMCS).⁵ It was demonstrated that antisense oligonucleotide-mediated downregulation of CIC-3 dramatically inhibits cell proliferation of rat aortic SMCs.¹⁹ The *CICn-3* gene appears to be upregulated in rat pulmonary artery and heart in response to monocrotaline-induced pulmonary hypertension and in canine cultured PASMCS incubated with inflammatory mediators. PASMCS infected to overexpress CIC-3 exhibited enhanced viability against H₂O₂, thus suggesting that CIC-3 may improve the resistance of VSMCs to reactive oxygen species (ROS) in an environment of elevated inflammatory cytokines in hypertensive pulmonary arteries.²⁰ These and other studies suggested that activation of CIC-3 channels may indeed play a role in proliferation, growth, volume regulation, and apoptosis of vascular SMCs (see Ref. ²¹ for review).

2 Properties of Native VSOACs in PASMCS

Quantitative reverse-transcription polymerase chain reaction (RT-PCR) has been used to test for molecular expression of CIC-3 in canine pulmonary smooth muscle. Primers were designed to be specific for CIC-3 and do not cross hybridize to other members of the CIC gene family. The competitive “mimic” strategy of quantitative PCR was employed.¹² As shown in Fig. 15.1a, quantitative RT-PCR detected significant levels of CIC-3 transcriptional expression from pulmonary arteries. The figure

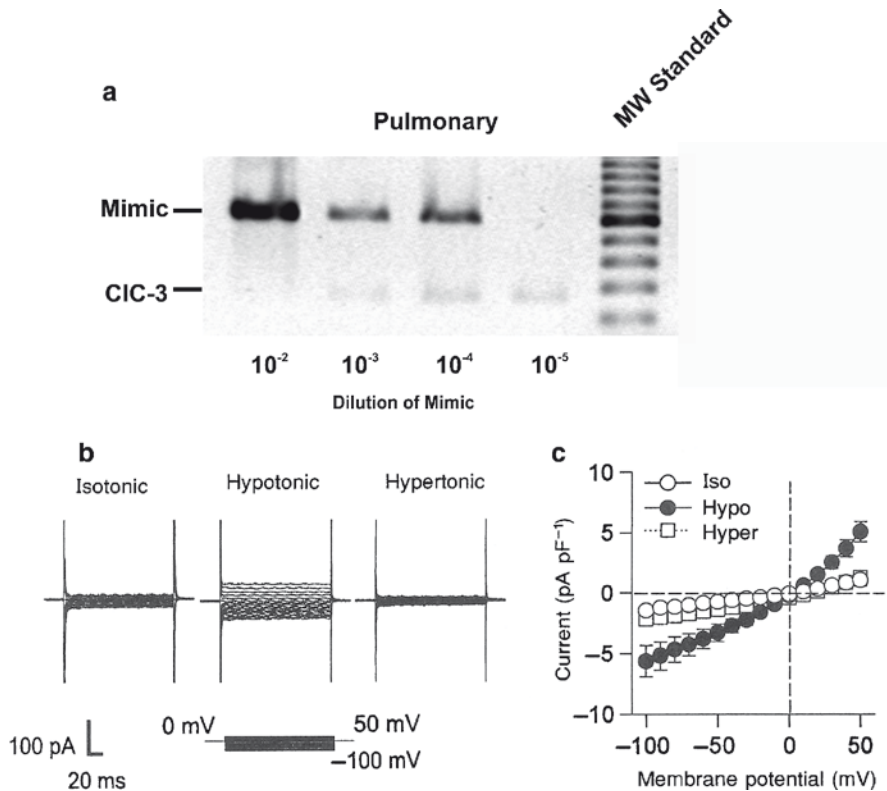


Fig. 15.1 CIC-3 expression and native VSOACs in canine PASMCS. (a) Representative gel of quantitative RT-PCR for CIC-3 in canine pulmonary arteries; competitive PCR products were resolved on 2% ethidium bromide agarose gels. Tenfold serial dilutions of mimic DNA were included in the PCRs, while target cDNA (CIC-3) concentration remained constant. The actual concentrations of target complementary DNA (cDNA) were calculated and expressed as percent of β -actin RNA concentration. (b) Raw VSOAC currents activated by hypotonic solutions during 150-ms voltage steps from 0 mV to potentials ranging from -100 to 50 mV. The cell was first equilibrated with the isotonic solution and then exposed to the hypotonic solution. Activations of VSOACs were reversed by exposure to hypertonic solutions. (c) Current-voltage relations for volume-regulated currents in the isotonic, hypotonic, and hypertonic solutions with $115 \text{ mM } [\text{Cl}]_o$ and $115 \text{ mM } [\text{Cl}]_i$ ($n = 4$). Modified with permission⁵

illustrates a representative gel used in digital analysis and comparison of mimic and CIC-3 amplification. Digital analysis and comparison of mimic and CIC-3-specific amplification products was performed on the 10^{-4} dilution of mimic DNA and was repeated on three independently generated samples. CIC-3 expression was 48.0% of β -actin in pulmonary artery. Figure 15.1b, c illustrate the activation of native VSOACs in canine PASMCS by exposure to hypotonic (230 mOsm) extracellular solutions. Exposure to a hypotonic solution causes cells to swell, which results in the delayed activation of VSOACs. Membrane currents at -100 and $+100$ mV were almost negligible in the isotonic solution but began to increase following a delay of some 3–4 min after changing to the hypotonic solution. Figure 15.1b shows raw

current traces evoked by step pulses, which developed during exposure to hypotonic solution, and these were completely abolished by a 10-min perfusion with a hypertonic solution. In these experiments, possible contamination by cation currents was prevented using impermeant cations and appropriate blockers. Figure 15.1c is a plot of the current–voltage relations obtained from several cells in solutions with different osmolarities. In these experiments, both bath and pipet solutions contained 115 mM Cl⁻, and the currents activated during exposure to hypotonic solution exhibited clear outward rectification. The reversal potential was approximately 0 mV, which is the predicted equilibrium potential for Cl⁻ (0 mV). The hypotonically activated currents were reduced by subsequent exposure to hypertonic solutions at each membrane potential. Membrane currents activated by exposure to hypotonic solutions were also markedly inhibited by the stilbene compound DIDS (4,4'-diisothiocyanatostilbene-2,2'-disulphonic acid).

Figure 15.2 illustrates the effects of intracellular dialysis with an anti-CIC-3 carboxyl terminus antibody (C₆₇₀₋₆₈₇ Ab) on native VSOAC currents in PSMCs. Membrane currents were obtained by applying 100-ms step pulses to ±80 mV from a holding potential of -40 mV every 30 s. In Fig. 15.2a, b, the time courses of change in the amplitudes of membrane currents measured at ±80 mV are shown, and original current traces obtained at the time points indicated by small letters are depicted in the insets. In a cell dialyzed with 10 μg mL⁻¹ C₆₇₀₋₆₈₇ Ab for over 10 min, basal membrane currents gradually declined in isotonic bath solution. Subsequent hypotonic cell swelling failed to induce any increase of the current amplitude (Fig. 15.2a). To know whether the observed inhibitory effects of C₆₇₀₋₆₈₇ Ab on VSOACs were due to specific binding, similar experiments were repeated with the

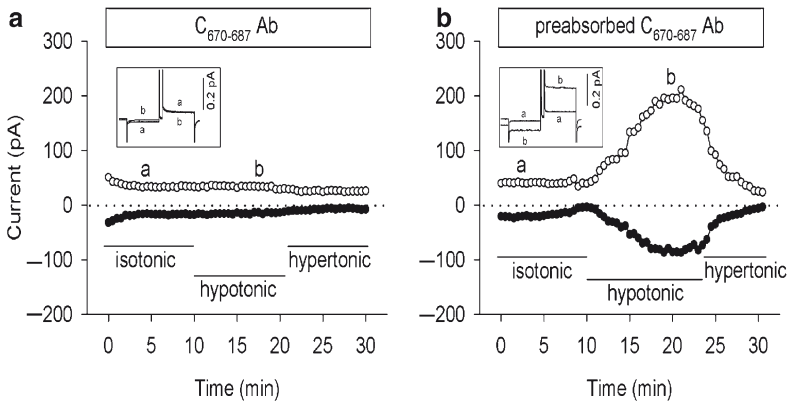


Fig. 15.2 Inhibition of native VSOACs in canine PSMCs by anti-CIC-3 C₆₇₀₋₆₈₇ Ab intracellular dialysis. Membrane currents were induced by repetitive 100-ms voltage steps to ±80 mV from a holding potential of -40 mV every 30 s. (a, b) Time courses of change in current amplitude measured at both -80 mV (filled circles) and +80 mV (open circles) in two representative cells intracellularly dialyzed with either 10 μg mL⁻¹ CIC-3 C₆₇₀₋₆₈₇ Ab (a) or the antigen-preabsorbed C₆₇₀₋₆₈₇ Ab (b). The bars underneath the current traces indicate different bath solutions. Original current recordings obtained at the time points indicated by small letters are shown in the corresponding insets. Modified with permission³²

antigen-preabsorbed $C_{670-687}$ Ab. Figure 15.2b shows a representative experiment. In contrast to the effects observed with the $C_{670-687}$ Ab alone, dialysis with $10 \mu\text{g mL}^{-1}$ antigen-preabsorbed $C_{670-687}$ Ab for over 10 min did not prevent activation of VSOACs on hypotonic cell swelling. Subsequent exposure of the cell to hypertonic bath solution totally reversed the swelling-induced VSOAC currents.

3 Anion Selectivity of Native VSOACs in PASMCs and sCLC-3 Heterologously Expressed in NIH/3T3 Cells

To examine Cl^- dependence, the reversal potentials E_{rev} for the volume-sensitive currents were measured using either voltage steps or ramps in hypotonic solutions containing six different concentrations of external Cl^- ($[\text{Cl}^-]_o$), replaced with aspartate. As shown in Fig. 15.3a, reducing $[\text{Cl}^-]_o$ from 115 to 28 and 9 mM shifted E_{rev} rightward, indicating a strong Cl^- dependence of the volume-sensitive conductance. The inset shows the relationship between $[\text{Cl}^-]_o$ and E_{rev} of the volume-sensitive conductance obtained from a number of pulmonary cells. The straight line represents a theoretical slope of 57 mV per tenfold decrease in $[\text{Cl}^-]_o$, which is predicted from the Nernst equation assuming that Cl^- is the only permeable ion. The slope of the relationship measured experimentally closely followed the predicted slope of 57 mV per tenfold change in $[\text{Cl}^-]_o$ for changes in $[\text{Cl}^-]_o$ greater than 40 mM but deviated

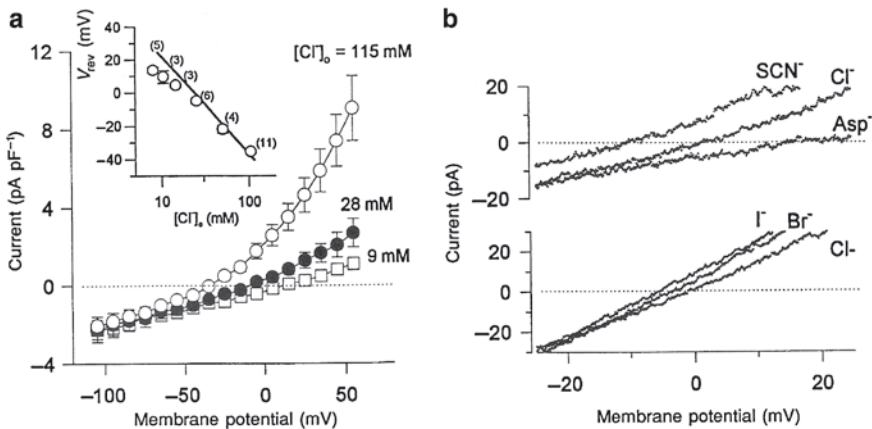


Fig. 15.3 Effect of $[\text{Cl}^-]_o$ (a) and anion substitution (b) on current-voltage relations of VSOAC currents elicited in canine pulmonary arterial smooth muscle cells by voltage steps or ramps. (a) The pipet solution contained 24 mM Cl^- ($n = 5$). *Inset*, relation between the reversal potential (E_{rev}) and $[\text{Cl}^-]_o$. Each circle indicates the mean value of E_{rev} with standard errors of the means (SEM) from N observations indicated in the parentheses. The straight line indicates the theoretical slope of 57 mV per tenfold decrease in $[\text{Cl}^-]_o$, which is predicted from the Nernst equation. (b) NaCl (115 mM) in the bath solution was entirely replaced with the same concentration of NaI, NaBr, NaSCN, or Na aspartate. The pipet solution contained 115 mM Cl^- . Modified with permission⁵

from the predicted slope at $[Cl^-]_o$ less than 40 mM, suggesting that the replacement anion, Asp^- , may exhibit some limited permeability through these channels.

Relative anion selectivity was determined by total replacement of Cl^- with other anions in the hypotonic solutions. Figure 15.3b shows typical hypotonically activated membrane currents elicited in a pulmonary cell by voltage ramps applied in the presence of different extracellular anions. I^- appeared to be slightly more permeable, compared to Br^- , which was more permeable than Cl^- in this example. Likewise, SCN^- appeared to be more permeable compared to Cl^- , which was more permeable than aspartate $^-$. The mean data accumulated from a group of cells gave E_{rev} values (in mV) of -8.29 ± 0.92 ($n = 7$), -4.67 ± 1.49 ($n = 12$), -3.30 ± 1.16 ($n = 10$), 0.46 ± 1.01 ($n = 13$) and 12.40 ± 1.69 ($n = 5$) for SCN^- , I^- , Br^- , Cl^- and aspartate $^-$, respectively. Accordingly, the relative permeability for each anion (X^-) to Cl^- (P_{X^-}/P_{Cl^-}) was estimated using the Goldman-Hodgkin-Katz equation. The sequence of (P_{X^-}/P_{Cl^-}) was SCN^- (1.36 ± 0.06) > I^- (1.19 ± 0.06) > Br^- (1.09 ± 0.04) > Cl^- (1.00) > aspartate $^-$ (0.63 ± 0.05). These data indicate that these membrane currents activated by hypotonic cell swelling in PSMCs can be identified as VSOACs.

sCIC-3 has been successfully expressed in NIH/3T3 cells⁴ and in A10 vascular SMCs.¹¹ In both cell types, sCIC-3 transfection gives rise to larger volume-sensitive Cl^- currents, compared to untransfected cells, with properties resembling those of native VSOACs. VSOACs in A10 sCIC-3-transfected cells are completely abolished by intracellular dialysis of an anti-CIC-3 antibody and by CIC-3 antisense oligonucleotides.

We have examined the relative anion selectivity of expressed sCIC-3 currents in NIH/3T3 cells to determine if it is similar to the anion permeability properties of native VSOACs in canine PSMCs (cf. Fig. 15.3). The results of these experiments are summarized in Table 15.1. To measure relative whole-cell anion permeability, external NaCl was replaced by the sodium salt of various anions. Reversal potentials were measured for each Cl^- substitute (X) and the relative shifts in reversal potential ($E_X - E_{Cl}$) were used to calculate the relative permeability ratio (P_X/P_{Cl}) for each anion. The relative anion permeability (P_X/P_{Cl}) of expressed sCIC-3 currents activated by hypotonic cell swelling was SCN^- (1.50) > I^- (1.34) > NO_3^- (1.27) > Br^- (1.15) > Cl^- (1.00) > F^- (0.57) > isethionate(0.25) > gluconate(0.09). These

Table 15.1 Relative anion selectivity of sCIC-3 channels expressed in NIH 3T3 cells

| Anions | $E_X - E_{Cl}$ | P_X/P_{Cl} | n |
|-------------|------------------|-----------------|-----|
| SCN^- | -9.30 ± 2.03 | 1.50 ± 0.14 | 5 |
| I^- | -6.89 ± 0.86 | 1.34 ± 0.05 | 5 |
| NO_3^- | -5.50 ± 1.22 | 1.27 ± 0.07 | 5 |
| Br^- | -3.36 ± 0.42 | 1.15 ± 0.02 | 5 |
| Cl^- | 0 | 1.0 | |
| F^- | 13.03 ± 0.99 | 0.57 ± 0.02 | 5 |
| Isethionate | 32.27 ± 4.29 | 0.25 ± 0.05 | 5 |
| Gluconate | 49.61 ± 4.15 | 0.09 ± 0.02 | 5 |

results demonstrate that sCIC-3 channels exhibit a lyotropic anion permeability similar to native VSOACs in PSMCs and most mammalian cells.¹

4 Do Native VSOACs in PSMCs and Heterologously Expressed sCIC-3 Behave as Chloride/Proton Antiporters?

The molecular structure of the CIC family of voltage-gated proteins has been determined by X-ray crystallography of the bacterial homologue EcCIC.^{22, 23} EcCIC is a homodimer with each subunit consisting of 18 α -helical transmembrane-spanning domains and a cytoplasmic domain containing two cystathionine β -synthetase (CBS) subdomains. A selectivity filter has been identified that contains three selective anion-binding sites.²⁴ Surprisingly, a study²⁵ demonstrated that the bacterial homologue EcCIC functions as an H^+ - Cl^- -exchange transporter, not as an ion channel. This was convincingly demonstrated since membrane currents associated with EcCIC are relatively voltage independent and changes in proton gradients produced easily measurable shifts in current reversal potential, as predicted for an exchange transport mechanism. Efforts have been made to extend these results to the mammalian family of CIC Cl^- channels. Conservation of a putative “proton” glutamate (Glu-203) in the selectivity region between EcCIC and the mammalian homologues CIC-3–CIC-7 has suggested the possibility that these proteins may also function as proton exchange transporters.²⁶ The major evidence for this proposal is indirect and comes from studies heterologously expressing CIC-4 and CIC-5. The difficulty is that expressed CIC-4 and CIC-5 currents exhibit strong outward rectification, making it impossible to measure reversal potentials or shifts in reversal potentials with changes in extracellular anion or proton concentrations. As an alternative approach, changes in intracellular pH were measured in CIC-4- and CIC-5-transfected tsA201 cells²⁷ or changes in extracellular pH in CIC-4- and CIC-5-transfected oocytes²⁸ to monitor proton fluxes attributable to electrogenic Cl^-/H^+ exchange.

We have examined whether native VSOACs in cultured canine PSMCs behave as Cl^- channels or as Cl^-/H^+ antiporters. As shown in Fig. 15.4a, VSOAC currents activated by hypotonic cell swelling in canine PSMCs were strongly inhibited at both positive and negative membrane potentials when the extracellular hypotonic solution pH was changed from 7.3 to 4.5. Raw traces of VSOAC currents recorded over the voltage range -100 to $+100$ mV are illustrated in Fig. 15.4b, c. Figure 15.4d shows the current-voltage relationships of VSOACs recorded in the presence of hypotonic (pH 7.3) solutions and hypotonic (pH 4.5) solutions for a number of cells. Both inward and outward VSOAC currents were inhibited by extracellular acidification; significantly, there was no observed change in membrane current reversal potential.

If the transport mechanism involves Cl^-/H^+ exchange, the membrane current reversal potential V_r is defined by the following equation²⁵:

$$V_r = (E_{Cl} + rE_H) / (1 + r)$$

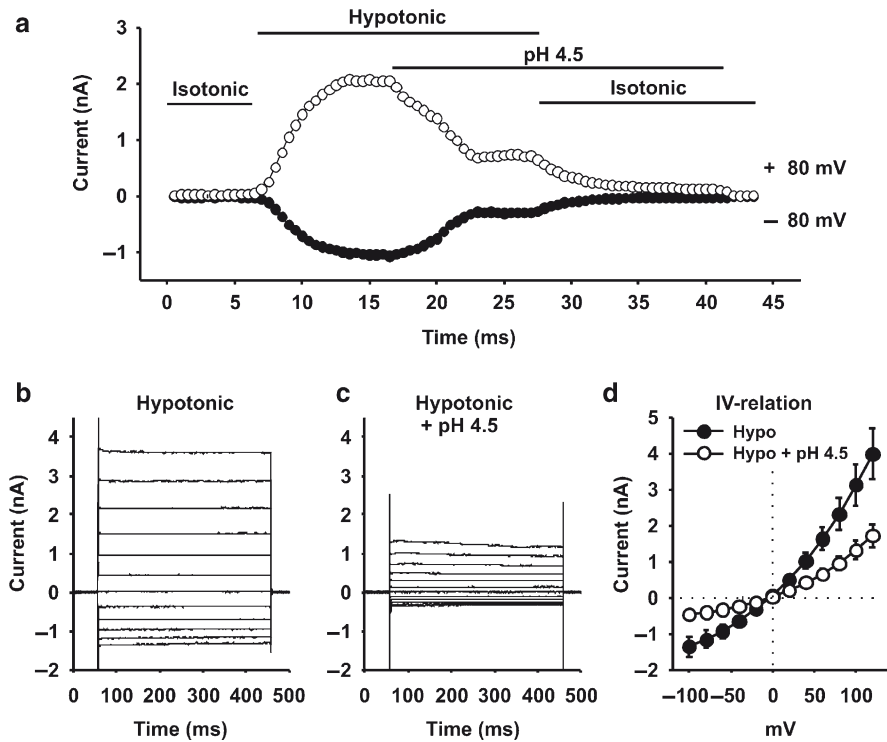


Fig. 15.4 Inhibition of VSOACs by extracellular acidification in cultured canine PSMCs. (a) Time course of membrane currents activated at ± 80 mV by hypotonic (230 mOsm, pH 7.4) solution. Following maximal activation, the extracellular solution was changed to a hypotonic (230 mOsm, pH 4.5) solution at the time indicated by the horizontal bars. External acidification inhibited both outward and inward VSOAC currents, and the remaining currents were reversed by reexposure to isotonic solution. Traces of membrane currents elicited by voltage steps over the range -100 to +125 mV in hypotonic (230 mOsm, pH 7.4) solution (b) and after changing to a hypotonic (230 mOsm, pH 4.5) solution (c). (d) Current-voltage (IV) relationships of membrane currents shown in (b, c). Extracellular acidification inhibited VSOACs without inducing any significant change in current reversal potential (G.-X. Wang and J.R. Hume unpublished data)

where E_{Cl} is the equilibrium potential for Cl^- , E_{H} is the equilibrium potential for protons, and r is the proton-anion coupling ratio. For a Cl^-/H^+ exchange transport protein, significant changes in the proton gradient should produce measurable changes in the membrane current reversal potential, which we failed to observe (Fig. 15.4d) for native VSOACs in PSMCs. This is quite different from the findings on the bacterial homologue EcCIC, for which extracellular acidification produced a negative shift in measured reversal potentials.²⁵

We have also examined whether hsCIC-3 currents measured in transfected NIH/3T3 cells behave as Cl^- channels or as Cl^-/H^+ antiporters. As shown in Fig. 15.5a, b, hypotonically activated hsCIC-3 currents were significantly inhibited by extracellular acidification. Extracellular acidification produced no measurable change in hsCIC-3 current reversal potential (Fig. 15.5c), suggesting that hsCIC-3

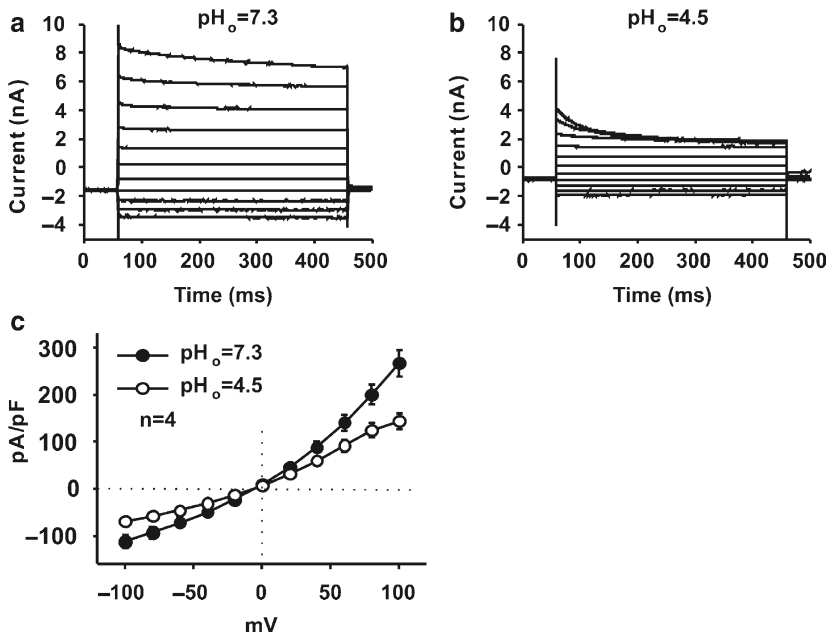


Fig. 15.5 Effect of extracellular acidification on hsCIC-3 currents in transfected NIH/3T3 cells. Traces of membrane currents elicited by voltage steps over the range ± 100 mV in hypotonic (230 mOsm, pH 7.4) solution (**a**) and after changing to a hypotonic (230 mOsm, pH 4.5) solution (**b**). (**c**) Current-voltage (IV) relationships of membrane currents shown in (**a**, **b**). hsCIC-3 currents were inhibited by extracellular acidification, but acidification had no effect on membrane current reversal potential (G.-X. Wang and J.R. Hume unpublished data)

exhibits properties more consistent with a Cl^- channel electrodiffusion mechanism compared to a Cl^-/H^+ countertransport mechanism.

5 Summary and Conclusions

Native VSOACs in cardiac and SMCs share many properties with recombinant sCIC-3 channels expressed in heterologous expression systems, including outwardly rectifying Cl^- currents activated by cell swelling and inhibited by cell shrinkage; current inhibition at strong positive membrane potentials; and inhibition by extracellular nucleotides, stilbene derivatives such as DIDS and 4-Acetamido-4'-isothiocyanato-2,2'-stilbenedisulfonic acid (SITS), intracellular dialysis by anti-CIC-3 antibodies and by the antiestrogen compound tamoxifen.²⁹ Moreover, as shown in this chapter, native VSOACs in PASMCS and expressed recombinant cCIC-3 channels exhibit a similar lyotropic permeability selectivity of $\text{SCN}^- > \text{I}^- > \text{NO}_3^- > \text{Br}^- > \text{Cl}^- > \text{F}^- > \text{isethionate} > \text{gluconate}$. Despite suggestions that some members of the mammalian CIC Cl^- channel family may function as chloride/proton

antiporters like the bacterial homologue EcClC, membrane current reversal potential measurements on native VSOACs in PSMCs and recombinant sClC-3 currents failed to provide any evidence supporting a role for chloride/proton antiporter function.

Native VSOACs and ClC-3 have been implicated in a wide variety of SMC functions, including proliferation, growth, apoptosis, and protection against oxidative stress. It is possible that all of these might be explained by the role that VSOACs and ClC-3 normally play in normal cell volume homeostasis. However, it is possible that an important physiological function of these channels may extend beyond their normal role in cell volume regulation.³⁰ For example, it has been demonstrated³¹ that ClC-3 Cl⁻ channels in the endothelial cell plasma membrane may be a prominent route for transmembrane flux of ROS. Future studies will certainly focus on such a possibility in PSMCs.

Acknowledgments Our work was supported by National Institutes of Health grants HL-49254 and P20RR1581 from the National Center for Research Resources.

References

1. Nilius B, Droogmans G (2003) Amazing chloride channels: an overview. *Acta Physiol Scand* 177:119–147
2. Voets T, Wei L, De Smet P et al (1997) Downregulation of volume-activated Cl⁻ currents during muscle differentiation. *Am J Physiol* 272:C667–C674
3. Nelson M, Conway MA, Knot HJ, Brayden JE (1997) Chloride channel blockers inhibit myogenic tone in rat cerebral arteries. *J Physiol* 502(2):259–264
4. Duan D, Winter C, Cowley S, Hume JR, Horowitz B (1997) Molecular identification of a volume-regulated chloride channel. *Nature* 390:417–421
5. Yamazaki J, Duan D, Janiak R, Kuenzli K, Horowitz B, Hume JR (1998) Functional and molecular expression of volume-regulated chloride channels in canine vascular smooth muscle cells. *J Physiol* 507:729–736
6. Do CW, Lu W, Mitchell CH, Civan MM (2005) Inhibition of swelling-activated Cl⁻ currents by functional anti-ClC-3 antibody in native bovine non-pigmented ciliary epithelial cells. *Invest Ophthalmol Vis Sci* 46:948–955
7. Jin NG, Kim JK, Yang DK et al (2003) Fundamental role of ClC-3 in volume-sensitive Cl⁻ channel function and cell volume regulation in AGS cells. *Am J Physiol Gastrointest Liver Physiol* 285:G938–G948
8. Petrunikina AM, Harrison RA, Ekhlasi-Hundrieser M, Topfer-Petersen E (2004) Role of volume-stimulated osmolyte and anion channels in volume regulation by mammalian sperm. *Mol Hum Reprod* 10:815–823
9. Vessey JP, Shi C, Jollimore CA et al (2004) Hyposmotic activation of I_{Cl} , swell in rabbit non-pigmented ciliary epithelial cells involves increased ClC-3 trafficking to the plasma membrane. *Biochem Cell Biol* 82:708–718
10. Wang L, Chen L, Jacob TJ (2000) The role of ClC-3 in volume-activated chloride currents and volume regulation in bovine epithelial cells demonstrated by antisense inhibition. *J Physiol* 524:63–75
11. Zhou JG, Ren JL, Qiu QY, He H, Guan YY (2005) Regulation of intracellular Cl⁻ concentration through volume-regulated ClC-3 chloride channels in A10 vascular smooth muscle cells. *J Biol Chem* 280:7301–7308

12. Jentsch TJ, Stein V, Weinreich F, Zdebek AA (2002) Molecular structure and physiological function of chloride channels. *Physiol Rev* 82:503–568
13. Li X, Shimada K, Showalter LA, Weinman SA (2000) Biophysical properties of CIC-3 differentiate it from swelling-activated chloride channels in Chinese hamster ovary-K1 cells. *J Biol Chem* 275:35994–35998
14. Weylandt KH, Valverde MA, Nobles M et al (2001) Human CIC-3 is not the swelling-activated chloride channel involved in cell volume regulation. *J Biol Chem* 276:17461–17467
15. Stobrawa SM, Breiderhoff T, Takamori S et al (2001) Disruption of CIC-3, a chloride channel expressed on synaptic vesicles, leads to a loss of the hippocampus. *Neuron* 29:185–196
16. Yamamoto-Mizuma S, Wang GX, Liu LL et al (2004) Altered properties of volume-sensitive osmolyte and anion channels (VSOACs) and membrane protein expression in cardiac and smooth muscle myocytes from $ClCn3^{-/-}$ mice. *J Physiol* 557:439–456
17. Xiong D, Wang G-X, Burkin D et al (2008) Cardiac specific overexpression of the human short CIC-3 chloride channel isoform in mice. *Clin Exp Pharmacol Physiol* 36:386–393, 2009
18. Lamb FS, Clayton GH, Liu BX, Smith RL, Barna TJ, Schutte BC (1999) Expression of CLCN voltage-gated chloride channel genes in human blood vessels. *J Mol Cell Cardiol* 31:657–666
19. Wang GL, Wang XR, Lin MJ, He H, Lan XJ, Guan YY (2002) Deficiency in CIC-3 chloride channels prevents rat aortic smooth muscle cell proliferation. *Circ Res* 91:e28–e32
20. Dai Y-P, Bongalon S, Hatton WJ, Hume JR, Yamboliev IA (2005) CIC-3 chloride channel is upregulated by hypertrophy and inflammation in rat and canine pulmonary artery. *Br J Pharmacol* 145:5–14
21. Guan YY, Wang GL, Zhou JG (2006) The CIC-3 Cl^{-} channel in cell volume regulation, proliferation and apoptosis in vascular smooth muscle cells. *Trends Pharmacol Sci* 27:290–296
22. Arianzi EA, Gpuld MN (1996) Identifying differential gene expression in monoterpenetreated mammary carcinomas using subtractive display. *J Biol Chem* 271:29286–29294
23. Dutzler R, Campbell EB, MacKinnon R (2002) X-ray structure of a CIC chloride channel at 3.0 Å reveals the molecular basis of anion selectivity. *Nature* 415:287–294
24. Dutzler R (2006) The CIC family of chloride channels and transporters. *Curr Opin Struct Biol* 16:1–8
25. Accardi A, Miller C (2004) Secondary active transport mediated by a prokaryotic homologue of CIC Cl^{-} channels. *Nature* 427:803–807
26. Zdebek AA, Zifarelli G, Bersforf E-Y et al (2008) Determinants of anion-proton coupling in mammalian endosomal CLC proteins. *J Biol Chem* 283:4219–4227
27. Scheel O, Zdebek AA, Lourdel S, Jentsch TJ (2005) Voltage-dependent electrogenic chloride/proton exchange by endosomal CLC proteins. *Nature* 436:424–427
28. Picollo A, Pusch M (2005) Chloride/proton antiporter activity of mammalian CLC proteins CIC-4 and CIC-5. *Nature* 436:420–423
29. Hume JR, Duan D, Collier ML, Yamazaki J, Horowitz B (2000) Anion transport in heart. *Physiol Rev* 80:31–81
30. Remillard CV, Yuan X-J (2005) CIC-3: more than just a volume-sensitive Cl^{-} channel. *Br J Pharmacol* 145:1–2
31. Hawkins BJ, Madesh M, Kirkpatrick CJ, Fisher AB (2007) Superoxide flux in endothelial cells via the chloride channel-3 mediated intracellular signaling. *Mol Biol Cell* 18:2002–2012
32. Wang G-X, Hatton WJ, Wang GL et al (2003) Functional effects of novel anti-CIC-3 antibodies on native volume-sensitive osmolyte and anion channels (VSOACs) in cardiac and smooth muscle cells. *Am J Physiol* 285:H1453–H1463